Oceanological and Hydrobiological Studies

International Journal of Oceanography and Hydrobiology

Volume 46, Issue 3, September 2017
pages (294-306)

ISSN 1730-413X
eISSN 1897-3191

Baltic Sea Holocene evolution based on OSL and radiocarbon dating: evidence from a sediment core from the Arkona Basin (the southwestern Baltic Sea)

by

Robert Kostecki[1,*], Piotr Moska[2]

DOI: **10.1515/ohs-2017-0031**
Category: **Original research paper**
Received: **July 11, 2016**
Accepted: **December 6, 2016**

[1] *Adam Mickiewicz University in Poznań, Institute of Geoecology and Geoinformation, Department of Quaternary Geology and Paleogeography, ul. Bogumiła Krygowskiego 10, 61-680 Poznań, Poland*

[2] *Silesian University of Technology, Institute of Physics, Department of Radioisotopes, GADAM Centre of Excellence, ul. Konarskiego 22B, 44-100 Gliwice, Poland*

* Corresponding author: *kostecki@amu.edu.pl*

Abstract

The paper presents the chronology of the Holocene evolution of the Baltic Sea based on the optically stimulated luminescence (OSL) and radiocarbon dating methods applied to a core taken from the Arkona Basin. The dating results were supplemented by grain size and geochemical analysis. The obtained results of OSL and radiocarbon dating enabled the construction of an age-depth model and confirmed the continuous sedimentation since 9900 cal yrs BP. One of the most interesting findings of this study is a clear relationship between the rate of sedimentation and fluctuations in the energy of depositional environment. The analyzed sediment core revealed two sections of different accumulation rates. The bottom section was deposited until 2700 cal yrs BP when the Ancylus Lake and the Littorina Sea were present, characterized by the accumulation rate estimated at around 0.46 mm year^{-1} and the dynamic sedimentation environment confirmed by grain size parameters. The accumulation rate at the top section deposited during the Post-Littorina Sea stage was estimated at around 1 mm year^{-1}. This stage, characterized by more stable deposition and lower-energy environment conditions, was confirmed by small grain size, symmetric skewness and increasing content of organic matter.

Key words: southern Baltic Sea, Arkona Basin, OSL, radiocarbon dating, grain size, Holocene, accumulation rate

DE GRUYTER

The *Oceanological and Hydrobiological Studies* is online at oandhs.ocean.ug.edu.pl

Introduction

The problem of the chronology of the Baltic Sea stages has been the subject of many studies (e.g. Jensen et al. 1999; Andrén et al. 2000; Moros et al. 2002; Borówka et al. 2005; Witkowski et al. 2005; Kortekaas 2007; Emelyanov & Vaikutienė 2015). The age of the beginning of particular stages and the rate of environmental changes vary across the Baltic basins. The high water level and salinity fluctuations controlled by glacioisotatic upward crustal movements and the eustatic sea level rise led to major changes in the environment of the Baltic Sea during the Holocene times. The results of these changes were the lacustrine and brackish-marine stages. The Baltic Ice Lake, the first stage of the Baltic Sea evolution, appeared in the study area soon after the deglaciation at ca. 16 000 cal yrs BP (Andren et al. 2011; Hughes et al. 2015) and existed until the final drainage at 11 600 cal yrs BP (Moros et al. 2002; Kortekaas et al. 2007). The Yoldia Sea was recorded in the Arkona Basin sediments as a short stage with low water levels and without marine influence (Moros et al. 2002). The following isostatic uplift of the Earth's crust and temperature increase led to isolation of the Baltic basin and the creation of the widespread freshwater Ancylus Lake with a water level at -19 m in the southern Baltic Sea (Jensen et al. 1999; Borzenkova et al. 2015). Traces of the maximum highstand of the Ancylus Lake dated around 10 300 cal yrs BP were found not only in the deepest parts of the Arkona Basin bottom (Rößler et al. 2011) but also in shallower southern parts of the basin off the Rugia island coast (Kostecki & Janczak-Kostecka 2011; 2012; Kostecki 2014). Soon after the maximum highstand, the water level of the Ancylus Lake in the study area dropped to -32 m as a result of lake drainage, presumably via the Dana River into the southern Kattegat (Lemke et al. 2001; Feldens & Schwarzer 2012; Bendixen et al. 2017). Clear indications of the initial Littorina Sea dated at ca. 8800 cal yrs BP were recognized only in Mecklenburg Bay sediments as a slightly brackish reservoir with weak marine inflows (Witkowski et al. 2005; Kostecki et al. 2015). The marine environment occurred first in Mecklenburg Bay at ca. 7500-7700 cal yrs BP and a few hundred years later at ca. 7200 cal year BP in the Arkona Basin (Rößler et al. 2011; Kostecki et al. 2015). The Littorina transgression in the Arkona Basin was described as the rapid change of environment from lacustrine to brackish-marine, confirmed by diatom and foraminifera analysis (Rößler et al. 2011; Kostecki & Janczak-Kostecka 2012). The last 3000 years of the Baltic Sea evolution, referred to as the Post-Littorina Sea stage, were characterized by a gradual reduction of marine influence, stable accumulation and depletion of oxygen in the water column (Andrén et al. 2000; Emelyanov & Vaikutienė 2013; Kostecki 2014).

Despite numerous studies dealing with the Baltic Sea evolution, the age of particular stages remains a matter of debate. The main problems with radiocarbon dating of the Baltic Sea stages were different dating materials and the inaccessibility of macrofossils. The most problematic issue is the age retrieved from the bulk sediments which, due to possible reworking with older carbon, yield dates around 1000 years too old (Kortekaas et al. 2007; Rößler et al. 2011). Calcareous fossils (especially bivalves in living positions) provide more accurate ages. Powerful currents and dynamic sedimentation often exclude the possibility of finding bivalve remains in the Littorina sediments. In such cases, it is possible to apply different dating methods. The optically stimulated luminescence (OSL) method of dating quartz samples has recently been used for the Baltic marine (Kortekaas et al. 2007) and coastal sediments (Jacobs 2008; Zhang et al. 2014). However, the results of the OSL dating method could be affected by an error caused by water content, compaction or partial bleaching. Thus, restrictions of both dating methods should be considered during the construction of a proper age-depth model.

The studied Arkona Basin is a shallow basin with an average water depth of 40-45 m, situated in the southwestern part of the Baltic Sea, close to the inlet area of the Great Belt and Øresund straits. Thus, the Arkona Basin is a suitable location for studies of the Baltic Sea evolution during the Holocene times. The characteristic feature of the morphology of the Arkona Basin is a flat bottom at isobaths below -40 m and several channels that connect the basin with the Danish straits and the adjacent Bornholm Basin.

The research was performed on the sediment core collected from the deepest part of the Arkona Basin to evaluate the grain size and geochemical composition, as well as the chronology was determined based on radiocarbon dating of macrofossils and OSL dating of quartz samples. The grain size distribution and geochemical composition are suitable for revealing changes in the depositional environment. The main objective of this study was to advance our knowledge about the accumulation rate, water level fluctuations and chronology of the Baltic Sea stages. Furthermore, changes in the accumulation compared to other basins of the southern Baltic Sea will be discussed.

Materials and methods

The gravity core EMB058-17-7 was retrieved from

the central part of the Arkona Basin aboard the research vessel FS "Elisabeth Mann Borgese" in 2013. The core was taken at a water depth of 46.3 m b.s.l. at 54°56.87'N and 13°18.20'E, 30 km to the north of Rugia Island (Fig. 1). The 6.68 m long core was cut into 1 m opaque tubes and stored in cool conditions. After opening, 10 OSL samples were taken from the core under amber light conditions. The sediments were described macroscopically. The core was subdivided into 1 cm samples, and geochemical and grain size analyses were performed at 2-5 cm intervals, depending on the lithology.

Geochemical and grain size analysis

Geochemical analyses of the core were conducted to determine the loss on ignition (LOI), and the content of terrigenous silica and biogenic silica. The loss on ignition was determined by combustion of dried sediment samples at 550°C, whereas the total silica content was determined by digestion of the combusted sample with aqua regia in a water bath lasting for 16 h at room temperature, followed by boiling for 2 h. Terrigenous silica content was determined by the residuals after dissolution of biogenic silica in a solution of 0.5 N sodium hydroxide. The grain size distribution was measured using the laser diffraction method with Malvern Mastersizer 2000. Carbon and organic matter were previously removed from the sediments with HCl and by boiling with H_2O_2 and washing with distilled water.

Radiocarbon dating

Shells and a bone were dated at the Poznań Radiocarbon Laboratory using ^{14}C accelerator mass spectrometry (AMS; Table 1). The radiocarbon dates from the lacustrine deposits were calibrated using the Intcal13 table (Reimer et al. 2013), while dates from the marine sediments were calibrated using Marine13 datasets (Reimer et al. 2013) with a reservoir age of 375 years based on the Chrono Marine Reservoir Database (Lougheed et al. 2013). The radiocarbon dates were calibrated with Calib6.11 software (Stuiver & Reimer 1993).

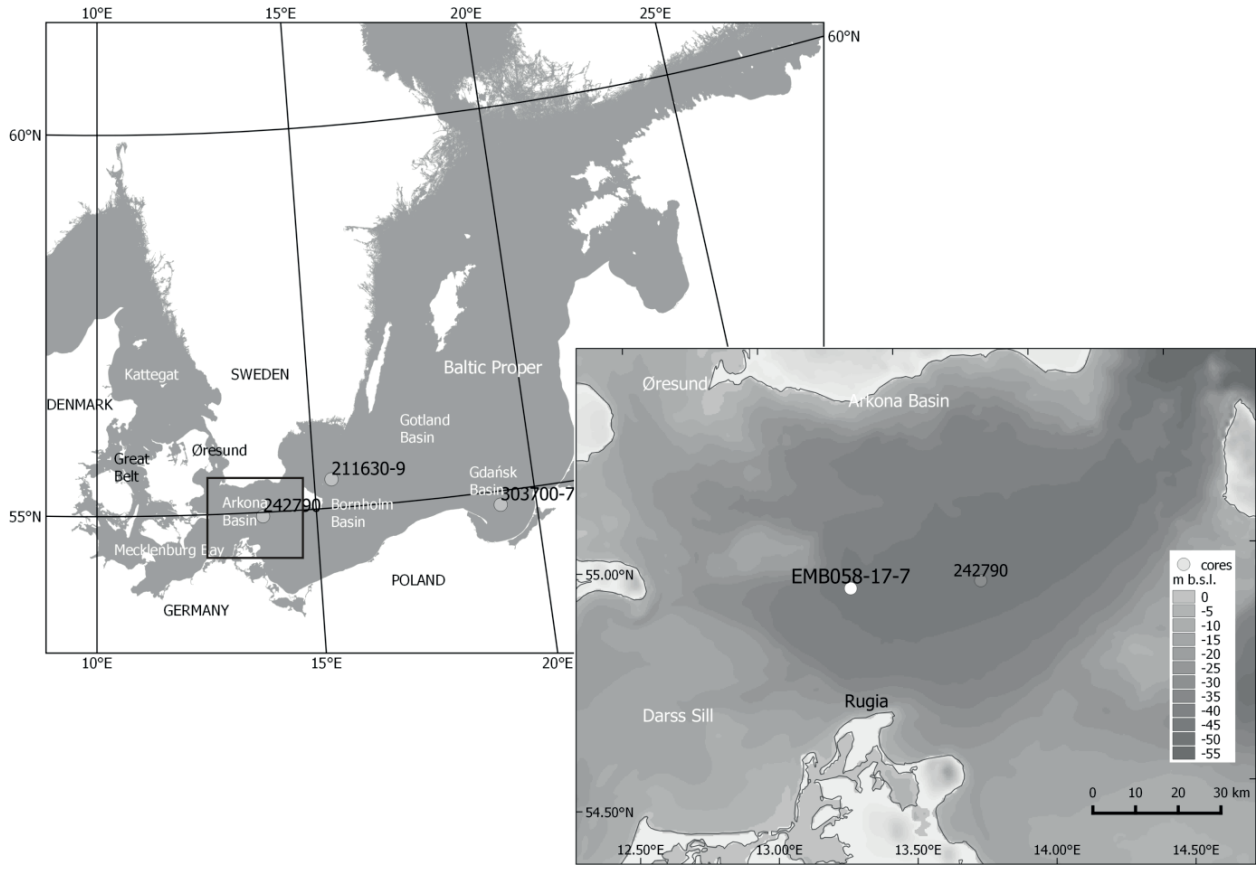

Figure 1

Location of the studied core (white circle) and previously published data (grey circles) presented in Table 3

Table 1

Results of AMS radiocarbon dating

Depth (cm)	Unit	Latitude	Longitude	Type of material	Radiocarbon age ^{14}C (BP)	Calibrated age 1 σ range; cal year BP(1950)	Laboratory code
85	U6	54°56.870´	13°18.200´	*Macoma* sp.	1070 ± 30	732 ± 97	Poz-62228
234	U5	54°56.870´	13°18.200´	*Macoma* sp.	2245 ± 30	1977 ± 128	Poz-62230
303	U5	54°56.870´	13°18.200´	*Macoma* sp.	2735 ± 30	2584 ± 130	Poz-62231
420	U3	54°56.870´	13°18.200´	fishbone	4600 ± 70	4986 ± 183	Poz-62232

OSL methodology

OSL dating was performed in the Gliwice Absolute Dating Method Centre, the Silesian University of Technology. Samples for OSL dating were taken from the marine core in laboratory conditions. The typical mass of the dry samples was between 50 and 100 g. The annual dose rates comprising beta and gamma radiation were calculated on the basis of gamma spectra measured in the laboratory using a dry sample. A Canberra spectrometer equipped with the HPGe detector was used for this purpose. Each measurement lasted about 24 h. Dose rates were calculated using the conversion factors of Adamiec and Aitken (1998). For the beta dose rate, the cosmic ray dose rate to the site was determined as described by Prescott and Stephan (1982). For each sample, we assumed that the average water content was similar to the values measured in our laboratory. For further calculations, a mean a-value of 0.04 ± 0.02 was assumed (Rees-Jones 1995). In the latter case, HF etching and grain size were taken into account (Fleming 1979). Beta dose attenuation was calculated using the method of Mejdahl (1979). Based on these data, the average dose rates for grain sizes of 90-125 and 125-200 µm were calculated (see Table 2). For standard OSL measurements, 90-125 and 125-200 µm grains of quartz were extracted from the sediment samples by a routine treatment with 20% hydrochloric acid (HCl) and 20% hydrogen peroxide (H_2O_2). The quartz grains were separated using density separation and applying sodium polytungstate solutions, leaving grains with densities between 2.62 and 2.75 g cm^{-3}. The grains were sieved before a 60 min etching with concentrated hydrofluoric acid (HF). Because our dating material comes from core (limited possibility of raw material), the number of quartz grains was also limited. This was particularly evident for the first five samples from EMB100 to EMB300. This is why our luminescence measurements were also limited to these samples (all possible material was used to calculate the final age; we have no possibility of re-measuring these samples). All OSL measurements were made using an automated Daybreak 2200 TL/OSL reader (Bortolot 2000). This reader uses blue diodes (470±4 nm) delivering about 60 mW cm^{-2} at the sample position. Laboratory irradiations were performed using a calibrated $^{90}Sr/^{90}Y$ beta source mounted onto the reader, delivering a dose rate of 3.0 Gy min^{-1}. For OSL measurements, a 6 mm Hoya U-340 filter was used.

Luminescence characteristics

For the investigated quartz fraction, equivalent doses were determined using the single-aliquot regenerative-dose (SAR) protocol (Murray & Wintle 2000). For equivalent dose calculation, the first second of the signal was used and the background was estimated from the final 10 s. The OSL SAR protocol used in our measurements consisted of the following steps:

1. Irradiation with the regenerative beta dose D_i
2. Preheat at 260°C for 10 s
3. Blue light stimulation at 125°C for 100 s
4. Irradiation with the test dose D_t (10% of the natural dose, but not less than 5 Gy)
5. Cut heat at 220°C
6. Blue light stimulation at 125°C for 100 s.

The intensities measured in steps 3 and 6 were used for equivalent dose determination. The SAR dose response curves were best represented by a single saturating exponential. A typical growth curve obtained for sample EMB400 is presented in Fig. 2, together with a typical decay curve. The ages were calculated using the Central Age Model (CAM: Galbraith et al., 1999) and are presented in Table 2 and Fig. 3, where relative probability density functions (Berger 2010) for all samples are presented. For some samples, the number of measured aliquots could not be increased because of the limitations in the amount of suitable material for luminescence measurements (samples EMB100, EMB150, EMB200, EMB250, EMB300).

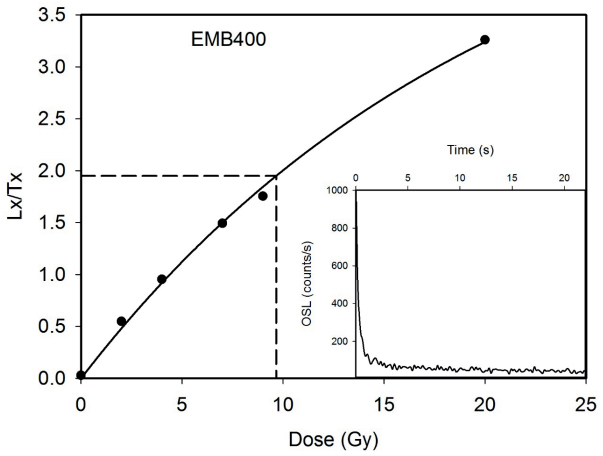

Figure 2

Typical dose response curves for sample EMB400 for quartz (OSL), together with a typical decay curve (insets)

Response curves were best fitted to a single saturating exponential. The dotted line presents a simple example of equivalent dose determination for one aliquot where Lx/Tx = 1.95 and D = 9.66 Gy.

We decided to use the CAM model to calculate the final results, because the overdispersion parameter of the distributions presented in Fig. 3 is lower than 20%; only sample EMB150 exceeds this value (but this is related to the fact that only four aliquots were measured for this sample).

A dose recovery test was carried out for five samples (EMB350, EMB400, EMB450, EMB480, EMB500; we did not have enough material for other samples): aliquots were bleached with blue light for 100 s (at room temperature) and after a pause of 10 000 s, they were bleached for another 100 s. After bleaching, a laboratory dose of a value similar to the equivalent dose of each sample (from 2-30 Gy – depending on the expected sample age) was administered and measured using the SAR protocol. In all cases, the dose recovery test performed for quartz grains using the standard SAR conditions yielded a ratio within the range of 0.9-1.1. A preheat plateau test was performed for sample EMB400. Preheat temperatures were varied from 200 to 300°C in 20°C steps. A slight effect of temperature on the equivalent dose was observed, but a higher value of D_e was observed for 300°C only. The results are presented in Fig. 4. This lack of systematic variation in the equivalent dose with preheat temperature also means that the thermal transfer from incompletely emptied traps should not be a problem. To control this recuperation parameter during our measurements, a 0 Gy regenerative dose step was incorporated into the SAR protocol (Murray & Wintle 2000). The intensity of recorded luminescence should be close to zero (this is known as the 'recuperated' luminescence signal). According to Murray and Olley (2002), recuperation should not be higher than 5% of the natural luminescence signal. The recuperation for all measured aliquots was lower than 5% during our investigation. Sensitivity changes during the SAR protocol are controlled and corrected using test doses that are an integrated part of the SAR procedure. The recycling ratio should be close to unity (Murray & Wintle 2000) and should not differ by more than 10%. These ratios were calculated for our samples, but we did not notice any strange behavior of the luminescence signal.

Table 2

Results of OSL dating

Sample	Depth (cm)	Unit	Lab. code	Age yrs BP	D_e (Gy)	n	^{238}U (Bq kg^{-1})	^{232}Th (Bq kg^{-1})	^{40}K (Bq kg^{-1})	Dose rate (Gy ka^{-1})	w.c.* (%)
EMB100	95-100	U6	GdTL-1957	1670 ± 140	1.63 ± 0.07	15	25.7 ± 0.6	37.6 ± 1.1	620 ± 21	0.94 ± 0.06	220 ± 10
EMB150	145-150	U6	GdTL-1956	1880 ± 400	1.98 ± 0.35	4	24.7 ± 0.7	39.3 ± 1.3	650 ± 23	1.05 ± 0.07	190 ± 10
EMB200	195-200	U5	GdTL-1955	4090 ± 390	5.8 5 ± 0.36	9	29.2 ± 0.4	40.2 ± 0.8	716 ± 23	1.43 ± 0.10	142 ± 10
EMB250	245-250	U5	GdTL-1954	2850 ± 260	3.94 ± 0.21	10	28.4 ± 0.4	36.4 ± 0.7	667 ± 21	1.38 ± 0.10	130 ± 10
EMB300	295-300	U5	GdTL-1953	3620 ± 350	5.25 ± 0.30	7	30.5 ± 0.6	39.5 ± 1.1	679 ± 23	1.45 ± 0.11	125 ± 10
EMB350	345-350	U4	GdTL-1952	4050 ± 390	6.69 ± 0.30	13	27.2 ± 0.5	31.2 ± 0.8	647 ± 21	1.65 ± 0.14	78 ± 10
EMB400	395-400	U3	GdTL-1951	5180 ± 490	9.74 ± 0.25	15	27.3 ± 0.5	29.0 ± 0.8	654 ± 21	1.88 ± 0.17	60 ± 10
EMB450	445-450	U3	GdTL-1950	7420 ± 650	15.1 ± 0.5	14	39.6 ± 0.5	42.8 ± 0.9	738 ± 24	2.04 ± 0.17	80 ± 10
EMB480	475-480	U2	GdTL-1949	9910 ± 780	23.2 ± 0.8	15	62.9 ± 0.8	68.8 ± 1.4	986 ± 33	2.34 ± 0.17	118 ± 10
EMB500	495-500	U1	GdTL-1948	12020 ± 1150	33.8 ± 0.8	14	49.3 ± 0.5	50.3 ± 0.8	834 ± 26	2.81 ± 0.26	53 ± 10

* w.c. - water content

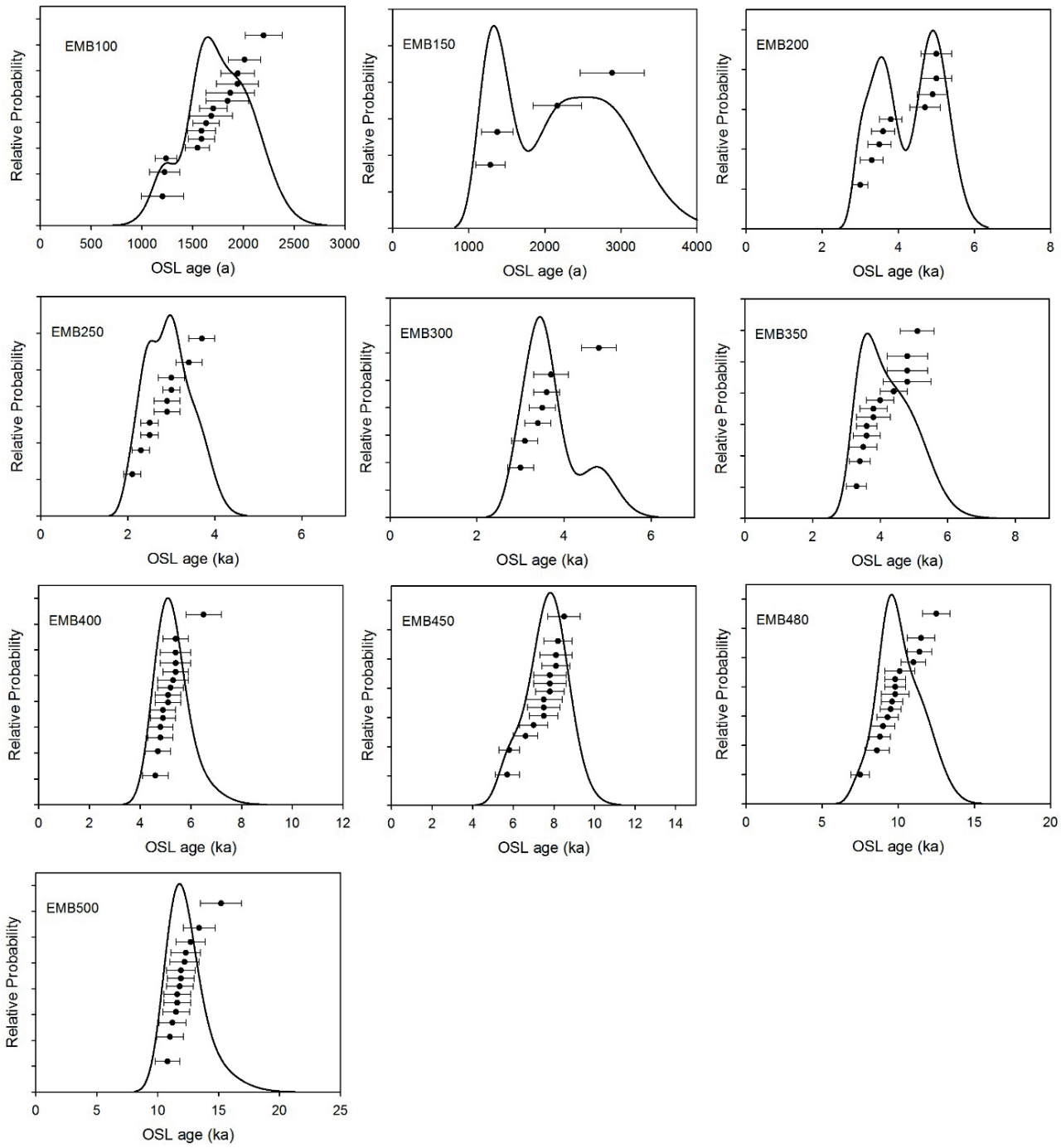

Figure 3

All luminescence results shown in graphs with relative probability density functions (Berger 2010)

Grain size parameter analyses

The grain size parameters were calculated using a computer program called GRADISTAT v.8 (Blott and Pye 2001). Folk (1966) graphical measures were applied to determine mean grain size (M_G), sorting (σ_G), skewness (Sk_G) and kurtosis (K_G). The analyzed core was subdivided into units based on the grain size distribution and the constrained hierarchical clustering algorithm by the method of the incremental sum of squares (Grimm 1987), implemented in the R package rioja (Juggins 2017). The number of significant

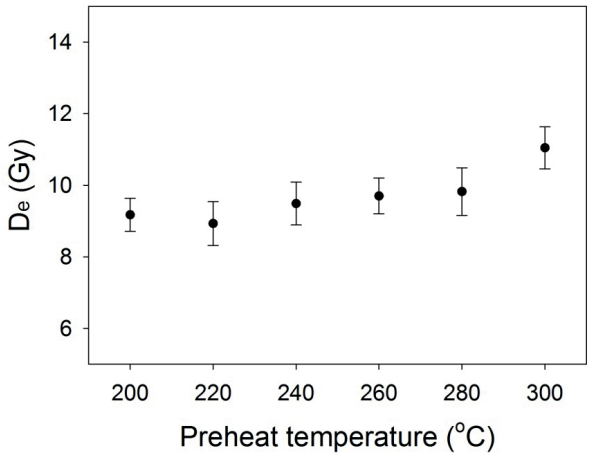

Figure 4

Preheat plateau test for sample EMB400

Each point represents the mean value from five independent aliquots that were measured for each preheat temperature.

units was determined by the broken-stick algorithm (Bennett 1996), also implemented in the rioja package (Juggins 2017).

Age-depth model calculations

The age-depth model was calculated using the Bacon program (Blaauw & Christen 2011) launched in the R environment. The accumulation rate was calculated according to values of the weighed mean age for each depth received as a result of calculations in the Bacon program.

Results

Lithology, geochemistry and grain size distribution

The analysis of grain size distribution and geochemistry was performed on the 0-500 cm section of the core EMB058-17-7 (Figs 5 and 6). The studied core was subdivided into six units based on the grain size distribution that related to changes in the lithology of the sediments. The lowermost unit U1 (500-492 cm) was identified in the light grey silty clay overlain by a 1 cm layer of light grey fine sand. These sediments were characterized by an upward increase in the mean grain size from medium silt to coarse silt (12.4-37.6 μm), poorly sorted (4.3-5.3), decreasing skewness form symmetrical to fine skewed (from 0.01 to -0.35), and platykurtic kurtosis (0.6-0.9). The top part of the unit was dominated by fine sand (47%). The sediments of this unit were also characterized by a low content of loss on ignition (4-6%) and biogenic silica (7-13%), and a high content of terrigenous silica (69-82%). The following unit U2 (492-450 cm) was recorded in the core section built of the dark olive-grey silt at the bottom and light grey silt at the top. The sediment of this unit was poorly sorted (4.6-3.7), medium silt (7-16 μm) with fluctuations of skewness from symmetrical to finely skewed (from 0.07 to -0.1) and slight fluctuations of kurtosis from mesokurtic to leptokurtic (0.91-1.01). A clear peak of mean grain size (13 μm) and an addition of medium and fine sand was recorded at a depth of 483 cm. The high content of loss on ignition (9-13%) and biogenic silica (16-18%), and an upward decrease in the content of terrigenous silica (62-48%) were characteristic geochemical

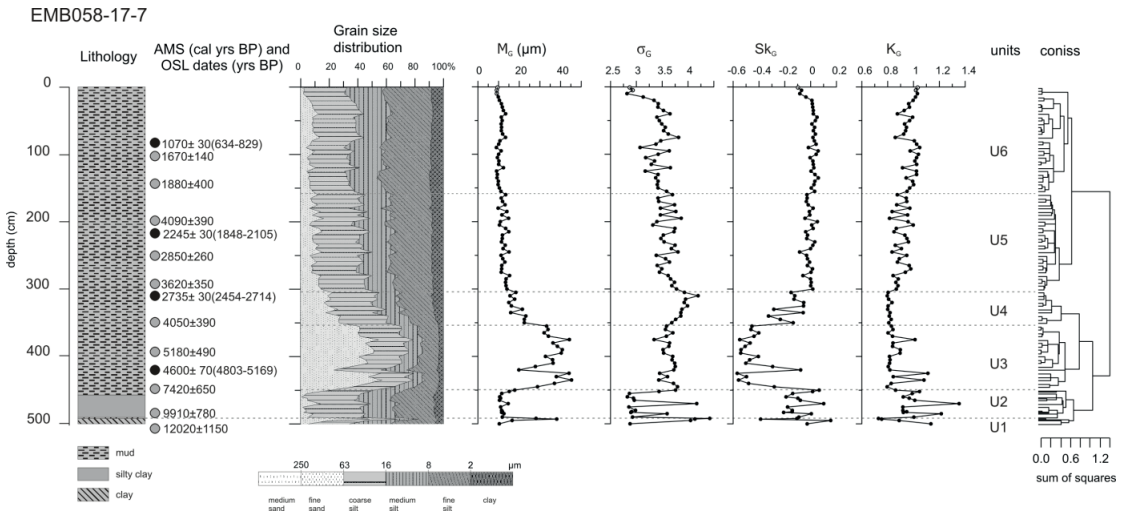

Figure 5

Grain size distribution and geochemical parameters in the studied core: black circles – radiocarbon dates; grey circles – OSL dates

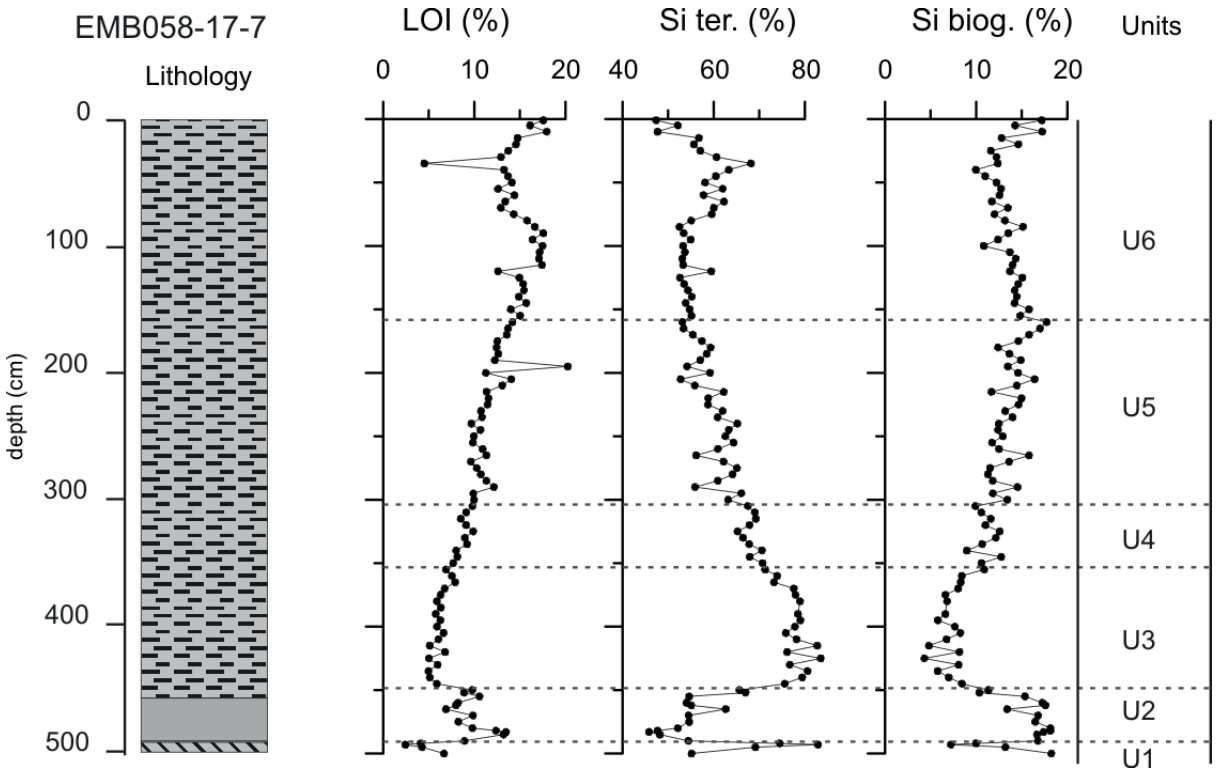

Figure 6

Geochemical parameters; lithology legend in Fig. 5

features of unit U2. The overlying unit U3 (450-355 cm) was formed from olive-grey sandy mud. In spite of the marine origin of the sediment of this unit, no mollusk shells were found. The grain size distribution of this unit described the sediment as poorly sorted (3.5), very coarse silt (20-31 μm), very finely skewed (from -0.3 to -0.4) and platykurtic (0.83-0.89). The main features of this unit were a strong increase in the mean grain size and the content of fine sand (from 12% to 57%). The geochemical parameters were characterized by a higher content of terrigenous silica (75-82%) and lower content of loss on ignition (4.9-7%) and biogenic silica (4-8%) compared to the underlying unit U2.

In unit U4 (355-305 cm), the olive-grey sandy mud was observed with an upward decrease in the mean grain size and increasing sorting and skewness. This sediment was described as being poorly sorted (3.6-3.9), coarse to medium silt (22-15 μm) with skewness from finely skewed to symmetrical (from -0.3 to -0.053) and platykurtic kurtosis (0.8). A few *Macoma sp.* shells were found in the upper part of the unit. Among the geochemical parameters, an upward increase in loss on ignition (7.6-9.8%) and biogenic silica (10-12%), and a decrease in terrigenous silica (70-65%) were observed. Unit U5 encompasses the sediment interval of 305-160 cm and was formed of olive-grey mud with abundant shells of *Macoma sp.* The grain size composition described sediment of this unit as poorly sorted (3.4-3.8), medium silt (10-14 μm) with symmetrical skewness (from -0.06 to 0.053) and kurtosis from platykurtic to mesokurtic (0.8-0.97). Similarly to the underlying unit U4, the value of loss on ignition and biogenic silica increased upward from 9.8% to 14.2% and from 11.8% to 17.7%, respectively. The content of terrigenous silica decreased upward from 66% to 53 %. The uppermost unit U6 (160-0 cm) was identified as olive-grey mud sediment. The color of the sediment was darker in the top 30 cm with a typical H_2S smell. Abundant shells of *Macoma* sp. were found in the core section of 152-83 cm. The sediment of this unit was characterized as medium silt (9-13 μm), poorly sorted (2.8-3.6) with symmetrical skewness (from -0.09 to 0.06) and mesokurtic kurtosis (0.87-1.0). The values of loss on ignition and the content of biogenic silica in unit U6 were 13-17% and 9-17%, respectively.

Age-depth model

The age-depth model presented in Fig. 7 was based on four radiocarbon dates retrieved from macrofossils (Table 1) and 10 OSL dates of quartz samples (Table 2).

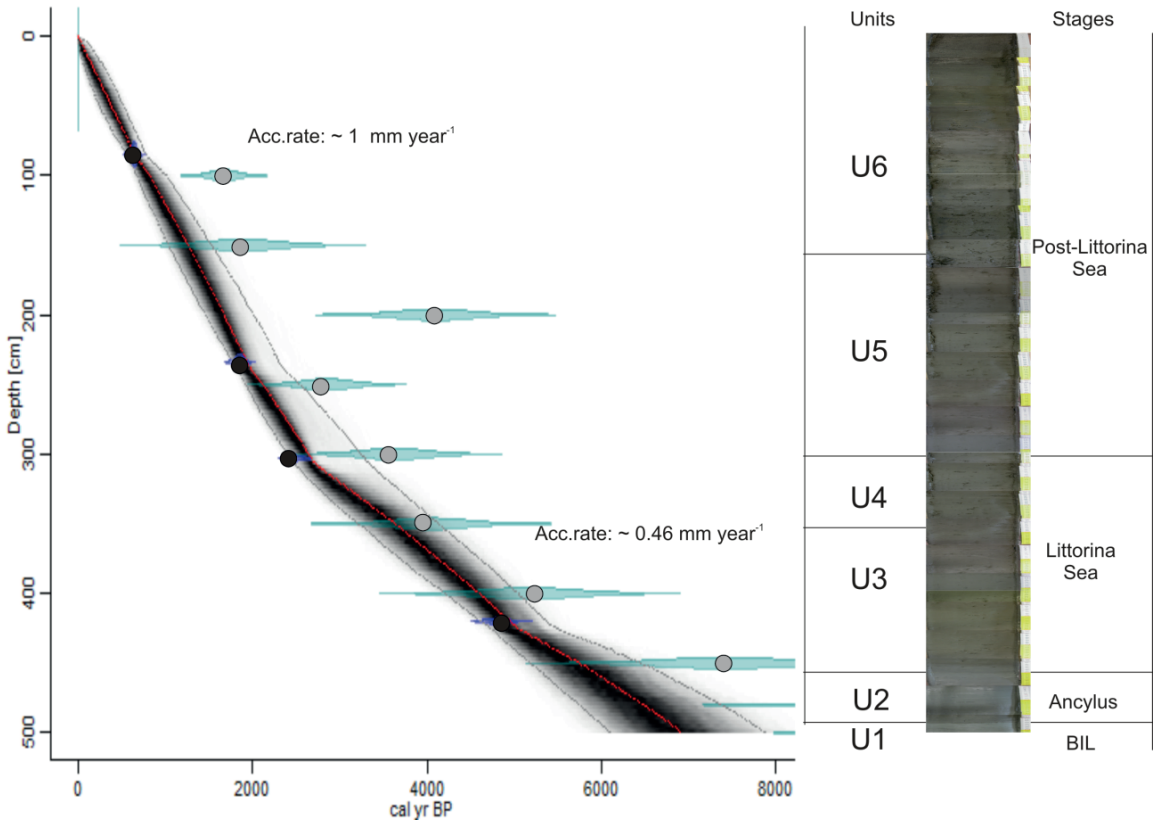

Figure 7

OSL and radiocarbon depth-age model plot: black circles – radiocarbon dates; grey circles – OSL dates, red curve – model based on the weighed mean age for each depth, grey stippled lines – 95% confidence intervals, transparent blue – uncertainty of ages

The OSL samples from depths of 480 and 500 cm are not presented due to their old age. The sample taken from unit U1 at a depth of 500 cm was OSL dated at 12 020 ± 1150 yrs BP. The thin layer of fine sand that overlaid the silty clay in unit U1 and the unexpectedly old age of sediment suggest the possibility of a hiatus, presumably at the top of this unit. The age of unit U2 deposition was estimated at the time interval between 9900 and 6500 cal BP based on two OSL dates of samples collected from depths of 480 cm and 450 cm. The radiocarbon date and three OSL dates retrieved from unit U3 allowed us to estimate the sediment deposition age at between 6500 and 3600 yrs BP. The macrofossil of a fishbone collected at a depth of 420 cm was dated at 4600 ± 70 ^{14}C years BP (4803-5169 cal yrs BP). The age of unit U4 sedimentation was estimated within the time span of 3600-2700 yrs BP according to two OSL dates and one radiocarbon date retrieved from a *Macoma* sp. shell. The overlying unit U5 was deposited in the time span of 2700-1500 yrs BP, while the uppermost unit U5 was related to the last 1500 yrs BP. The dates retrieved from *Macoma* sp. shells clearly correspond to the most OSL dates. The OSL date from the sample collected at a depth of 200 cm is too old and is overestimated due to possible partial bleaching or mixing with the older material. The mean accumulation rate (AR) was estimated at around 0.5 mm year^{-1}, but the core could be divided into two sections of different AR: ~0.46 mm year^{-1} for the bottom part of the core, and ~1 mm year^{-1} for the top part.

Discussion

Chronology of the Baltic Sea stages

The units distinguished based on the grain size distribution and geochemical composition supplemented by radiocarbon and the OSL age-depth model were assigned to respective Baltic Sea evolutionary stages. The bottom part of the

core in unit U1 consisted of silty clay covered by a thin sand layer. A similar layer of sand was found in previous investigations in other parts of the Arkona Basin (Moros et al. 2002; Kortekaas et al. 2007). The obtained OSL dates from a depth of 500 cm seem to be too old, but considering the abrupt change in the grain size distribution, we could conclude that this thin sand layer was presumably deposited during the final drainage of the Baltic Ice Lake at 11 600 cal yrs BP (Moros et al. 2002). This does not preclude the possibility of the hiatus in this part of the core. Continuous sedimentation in the studied core started with the silt of unit U2, dated at 9900 yrs BP. The retrieved age was around 11 200 cal yrs BP, suggesting that sediment of unit U2 was deposited after the Ancylus Lake regression (Jensen et al. 1999; Moros et al. 2002). Small grain size, symmetrical skewness and platykurtic kurtosis reflect a calm depositional environment with a low velocity of currents (Racinowski et al. 2001). As evidenced by the high content of loss on ignition and biogenic silica, such conditions were favorable for the development of organic production.

The most interesting Littorina transgression was represented by units U3 and U4. As evidenced by an abrupt increase in the mean grain size, decreasing skewness to very finely skewed and increasing addition of fine sand and terrigenous silica, the obtained depth-age model suggests that the main Littorina stage started at ~6000 cal yrs BP. These changes in grain size parameters reflect the intensification of a relatively high-energy environment, unstable deposition with high current velocities, and a tendency to redeposition during the first stage of the Littorina transgression. The age of the Littorina transgression culmination was estimated at around 5300 cal yrs BP and was confirmed by the peak of large mean grain size at a depth of 435 cm. A similar, relatively young date of the Littorina transgression in the Arkona Basin has been previously reported (Kortekaas et al. 2007; Rößler et al. 2011). Unit U3 reflects the most energetic depositional environment that existed in the Arkona Basin during the period of 6000-3600 cal yrs BP, controlled by strong inflows of saline waters from the Danish straits. After reaching the present water level at 4000 yrs BP (Winn and Averdieck 1984), the marine inflows into the Arkona Basin were reduced, reflecting a decrease in the mean grain size and increasing skewness toward the symmetrical one in unit U4. Organic sedimentation during the Littorina transgression was limited by the high energy of the environment. Such unfavorable environmental conditions were presumably responsible for the absence of calcareous fossils. The last 3000 cal yrs BP are represented by units U5 and U6, characterized by a small grain size, symmetric skewness and high mesokurtic kurtosis, reflecting a lower-energy environment and deceleration of currents with favorable conditions for deposition. The upward increasing content of biogenic silica and loss on ignition and the decreasing content of terrigenous silica confirmed these more favorable conditions for calmer sedimentation and primary production.

Comparing the retrieved age of the Littorina transgression in the Arkona Basin with the age of the first traces of the Littorina in Mecklenburg Bay, we can conclude that the first marine inflows occurred first in Mecklenburg Bay at ~8500 cal yrs BP via the Great Belt, as a slight and gradual change of environment (Kostecki et al. 2015). The increasing sea level led to the rapid inflow into the Arkona Basin at ~6000 cal yrs BP. Similar conclusions were reported by Rößler et al. (2011).

Reconstruction of the accumulation rate

The problem of changes in the accumulation rate during the Holocene times in the southern Baltic Sea has not been extensively discussed in the previous studies. The sediments analyzed in this study were deposited during the Littorina stage with different accumulation rates (Fig. 7). The bottom part of the core (500-300 cm) revealed a low accumulation rate, estimated at ~0.46 mm year^{-1}, whereas the accumulation rate in the top part of the core (300-0 cm) was higher, ~1 mm year^{-1}. The bottom section was deposited during 7000-2700 cal yrs BP and reflected an unstable depositional environment with major fluctuations in the water level and mineral material input. The depositional environment was controlled by strong currents that caused unfavorable conditions for sediment accumulation. The low accumulation rate was also confirmed by unfavorable conditions for biogenic production reflected by the low content of biogenic silica and loss on ignition. The upper section of the core deposited during the last 2700 years, related to the Post-Littorina Sea stage, revealed distinctly high accumulation in this part of the Arkona Basin. Comparing our results with others (Andrén et al. 2000; Kortekaas et al. 2007; Grigoriev et al. 2011; Emelyanov and Vaikutienė 2013), we conclude that the accumulation was spatially differentiated both within the Arkona Basin and in the whole southern Baltic Sea basin (Table 3). The common feature for the entire southern Baltic Sea is a similar fluctuation in the accumulation rate since the Ancylus Lake stage. The lower accumulation rate during the Ancylus Lake and the Littorina Sea was reported for the eastern part of the Arkona Basin (0.398 mm year^{-1}) by Kortekaas et al.

Table 3

Comparison of the accumulation calculation based on previous publications

Area	Lat. N, Long. E	Core	Duration (a)	Thickness (cm)	Sed. rate (mm year^{-1})	Publication
Arkona Basin	54.951°, 13.780°	242790	0-3600	225	0.625	Kortekaas et al. 2007
Arkona Basin	54.951°, 13.780°	242790	3600-8000	175	0.398	Kortekaas et al. 2007
Bornholm Basin	55.377°, 15.398°	211630-9	0-3000	325	1.083	Andrén et al. 2000
Bornholm Basin	55.377°, 15.398°	211630-9	3500-6550	228	0.48	Andrén et al. 2000
Gdańsk Basin	54.822°, 19.185°	303700-7	0-4800	205	0.427	Grigoriev et al. 2011
Gdańsk Basin	54.822°, 19.185°	303700-7	4800-9000	430	0.102	Grigoriev et al. 2011

(2007), for the Bornholm Basin (0.748 mm year^{-1}) by Andrén et al. (2000) and for the Gdańsk Basin (0.102 mm year^{-1}) by Grigoriev et al. (2011) and Emelyanov and Vaikutienė (2013). At the end of the Littorina Sea stage and during the Post-Littorina stage, the accumulation rate distinctly increased to 0.625 mm year^{-1} in the eastern part of the Arkona Basin, 1.083 mm year^{-1} in the Bornholm Basin and 0.427 mm year^{-1} in the Gdańsk Basin. The comparable result of the current accumulation rate in the Gdańsk Basin was estimated at 0.5-2 mm year^{-1} (Szmytkiewicz & Zalewska 2014).

Furthermore, the thickness of the sediments in the Arkona Basin deposited since the Littorina transgression also varies from 4.5 m (Moros et al. 2002; Kostecki and Janczak-Kostecka 2012; Kostecki 2014) in the western part to 3 m in the eastern part (Kortekaas et al. 2007). These varying thickness of the sediments between the western and eastern parts of the basin could be determined by the proximity to the channels that connect the basin with the Danish straits, providing inflows of more saline waters with suspended matter.

Conclusions

The obtained OSL and radiocarbon dates clarify our knowledge and confirm some of the previous results about the chronology of the Littorina transgression and dating methods. The OSL dating method allows us to estimate the age of sediments, despite the lack of organic material suitable for radiocarbon dating. The OSL method also excluded the problem with dating of the bulk sediment that yields overestimated results. The determined OSL ages were compared to radiocarbon dating results of marine fauna remains; a good fit was obtained. The obtained age-depth model allows us to confirm the age of the main Littorina transgression at ~6000 cal yrs BP in the Arkona Basin, and confirmed the suggestion of a rapid inflow of marine waters into this basin. The positive relation between the low accumulation rate and the increasing mean grain size confirmed the high-energy and unstable depositional environment during the Littorina transgression, as well as the more stable environment with higher deposition rates during the Post-Littorina Stage. The reasons behind the spatial differences in the accumulation rate across the entire southern Baltic Sea should be explained by future research.

Acknowledgements

We are grateful to Michael Endler and Rudolf Endler from the Leibniz Institute for Baltic Sea Research in Warnemünde for their help in obtaining the necessary material, and to Małgorzata Schade for sample preparation for laboratory analyses. The study was financed by the Polish National Science Centre within the framework of project 2011/01/B/ST10/06497. We thank Thomas Leipe and an anonymous reviewer for constructive comments.

References

Adamiec, G. & Aitken, M.J. (1998). Dose-rate conversion factors: update. *Ancient TL* 16: 37- 50.

Andrén, E., Andrén, T. & Sohlenius, G. (2000). The Holocene history of the southwestern Baltic Sea as reflected in a sediment core from the Bornholm Basin. *Boreas* 29: 233-250. DOI:10.1080/030094800424259.

Andren, T., Björck, S., Andren, E., Conley, D., Zillén, L. et al. (2011). The Development of the Baltic Sea Basin During the Last 130 ka. In *The Baltic Sea Basin* (pp. 75-97). Springer, Berlin Heidelberg.

Bendixen, C., Jensen, J.B., Boldreel, L.O., Clausen, O.R., Bennike,

O. et al. (2017). The Holocene Great Belt connection to the southern Kattegat, Scandinavia: Ancylus Lake drainage and Early Littorina Sea transgression. *Boreas* 46(1): 53-68. DOI: 10.1111/bor.12154.

Bennett, K.D. (1996). Determination of the number of zones in a biostratigraphical sequence. *New Phytol.* 132: 155-170.

Berger, G.W. (2010). An alternate form of probability-distribution plot for D_e values. *Antient TL* 28, 11-22

Blaauw, M. & Christen, J.A. (2011). Flexible paleoclimate age-depth models using an autoregressive gamma process. *Bayesian Analysis* 6: 457-474.

Blott, S.J. & Pye, K. (2001). GRADISTAT: a grain size distribution and statistics package for the analysis of unconsolidated sediments. *Earth Surf. Process. Landforms* 26: 1237-1248.

Borówka, R.K., Osadczuk, A., Witkowski, A., Wawrzyniak-Wydrowska, B. & Duda, T. (2005). Late Glacial and Holocene depositional history in the eastern part of the Szczecin Lagoon (Great Lagoon) basin--NW Poland. *Quat. Int.* 130: 87-96. DOI: 10.1016/j.quaint.2004.04.034.

Bortolot, V.J., (2000). A new modular high capacity OSL reader system. *Radiation Measurements* 32: 751-757.

Borzenkova, I., Zorita, E., Borisova, O., Kalniņa, L., Kisielienė, D. et al. (2015). Second assessment of climate change for the Baltic Sea Basin. In The BACC II Author Team (Eds.), *Second Assessment of Climate Change for the Baltic Sea Basin*. (pp. 25-49). Springer. DOI: 10.1007/978-3-319-16006-1.

Emelyanov, E.M. & Vaikutienė, G. (2013). Holocene environmental changes during tran sition Ancylus-Litorina stages in the Gdansk Basin, south-eastern Baltic Sea. *Baltica* 26: 71-82. DOI: 10.5200/baltica.2013.26.08.

Feldens, P. & Schwarzer, K. (2012). The Ancylus Lake stage of the Baltic Sea in Fehmarn Belt: Indications of a new threshold. *Cont. Shelf Res.* 35: 43-52. DOI: 10.1016/j.csr.2011.12.007.

Fleming, S. (1979). Thermoluminescence techniques in archaeology. Clarendon Press, Oxford.

Folk, R.L. (1966). A review of grain-size parameters. *Sedimentology* 6: 73-93. DOI: 10.1111/j.1365-3091.1966.tb01572.x.

Galbraith, R.F., Roberts, R.G., Laslett, G.M., Yoshida, H., Olley, J.M. (1999). Optical dating of single and multiple grains of quartz from Jinminum Rock Shelter, Northern 12 Australia. Part I, experimental design and statistical models. *Archaeometry* 41: 1835- 1857.

Grigoriev, A., Zhamoida, V., Spiridonov, M., Sharapova, A., Sivkov, V. et al. (2011). Late-glacial and Holocene palaeoenvironments in the Baltic Sea based on a sedimentary record from the Gdansk Basin. *Clim. Res.* 48: 13-21. DOI: 10.3354/cr00944.

Grimm, E.C. (1987). CONISS: a FORTRAN 77 program for stratigraphically constrained cluster analysis by the method of incremental sum of squares. *Comput. Geosci.* 13: 13-35. DOI: 10.1016/0098-3004(87)90022-7.

Hughes, A.L.C., Gyllencreutz, R., Lohne, Ø.S., Mangerud, J., Svendsen, J.I. (2015). The last Eurasian ice sheets - a chronological database and time-slice reconstruction, DATED-1. *Boreas* 45: 1-45. DOI: 10.1111/bor.12142.

Jacobs, Z. (2008). Luminescence chronologies for coastal and marine sediments. *Boreas* 37: 508-535. DOI: 10.1111/j.1502-3885.2008.00054.x.

Jensen, J.B., Bennike, O., Witkowski, A., Lemke, W. & Kuijpers, A. (1999). Early Holocene history of the southwestern Baltic Sea: the Ancylus Lake stage. *Boreas* 28: 437-453. DOI: 10.1111/j.1502-3885.1999.tb00233.x.

Juggins, S. (2017). rioja: Analysis of Quaternary Science Data, R package version (0.9-15). (http://cran.r-project.org/package=rioja).

Kortekaas, M. (2007). *Post-glacial history of sea-level and environmental change in the southern Baltic Sea. Lund University*. Department of Geology, Quaternary Sciences.

Kortekaas, M., Murray, A., Sandgren, P. & Björck, S. (2007). OSL chronology for a sediment core from the southern Baltic Sea: A continuous sedimentation record since deglaciation. *Quat. Geochronol.* 2: 95-101. DOI: 10.1016/j.quageo.2006.05.036

Kostecki, R. (2014). Stages of the Baltic Sea evolution in the geochemical record and radiocarbon dating of sediment cores from the Arkona Basin. *Oceanol. Hydrobiol. St*. 43: 237-246. DOI: 10.2478/s13545-014-0138-7.

Kostecki, R. & Janczak-Kostecka, B. (2011). Holocene evolution of the Pomeranian Bay environment, southern Baltic Sea. *Oceanologia* 53: 471-487.

Kostecki, R. & Janczak-Kostecka, B. (2012). Holocene environmental changes in the south-western Baltic Sea reflected by the geochemical data and diatoms of the sediment cores. *J. Mar. Syst*. 105-108: 106-114. DOI: 10.1016/j.jmarsys.2012.06.005.

Kostecki, R., Janczak-Kostecka, B., Endler, M. & Moros, M. (2015). The evolution of the Mecklenburg Bay environment in the Holocene in the light of multidisciplinary investigations of the sediment cores. *Quat. Int.* 386: 226-238. DOI: 10.1016/j.quaint.2015.07.007.

Lemke, W., Jensen, J.B., Bennike, O., Endler, R., Witkowski, A. et al. (2001). Hydrographic thresholds in the western Baltic Sea: Late Quaternary geology and the Dana River concept. *Mar. Geol.* 176: 191-201.

Lougheed, B.C., Filipsson, H.L. & Snowball, I. (2013). Large spatial variations in coastal 14C reservoir age – a case study from the Baltic Sea. *Clim. Past* 9: 1015-1028. DOI: 10.5194/cp-9-1015-2013.

Mejdahl, V. (1979). Thermoluminescence dating: beta-dose attenuation in quartz grains. *Archaeometry* 21, 1, pp. 61-72.

Moros, M., Lemke, W., Kuijpers, A., Endler, R., Jensen, J.B. et al. (2002). Regressions and transgressions of the Baltic basin reflected by a new high-resolution deglacial and postglacial lithostratigraphy for Arkona Basin sediments (western Baltic Sea). *Boreas* 31: 151-162. DOI: 10.1080/030094802320129953.

Murray, A.S. & Wintle, A.G. (2000). Luminescence dating of quartz using an improved singlealiquot regenerative-dose protocol. *Radiation Measurements* 32: 57-73.

Murray, A.S. & Olley, J.M. (2002). Precision and accuracy in the optically stimulated luminescence dating of sedimentary quartz: a status review. *Geochronometria* 21: 1-16.

Prescott, J.R. & Stephan, L.G. (1982). The contribution of cosmic radiation to the environmental dose for thermoluminescence dating. Latitude, altitude and depth dependencies. *TLS II-1*, pp. 16-25.

Racinowski, R., Szczypek, T. & Wach, J. (2001). *Prezentacja i interpretacja wyników badań uziarnienia osadów czwartorzędowych [Presentation and interpretation of the results of grain-size analysis]*. Silesian University, Katowice.

Rees-Jones, J. (1995). Optical dating of young sediments using fine-grain quartz. *Ancient TL*. 13: 9-14.

Reimer, P.J., Bard, E., Bayliss, A., Beck, J.W., Blackwell, P.G. et al. (2013). Intcal13 and marine13 radiocarbon age calibration curves 0-50,000 years cal BP. *Radiocarbon* 55: 1869-1887.

Rößler, D., Moros, M. & Lemke, W. (2011). The Littorina transgression in the southwestern Baltic Sea: new insights based on proxy methods and radiocarbon dating of sediment cores. *Boreas* 40: 231-241. DOI: 10.1111/j.1502-3885.2010.00180.x.

Stuiver, M. & Reimer, P.J. (1993). Extended 14C database and revised CALIB radiocarbon calibration program. *Radiocarbon* 35: 215-230.

Szmytkiewicz, A. & Zalewska, T. (2014). Sediment deposition and accumulation rates determined by sediment trap and 210Pb isotope methods in the outer puck bay (Baltic Sea). *Oceanologia* 56: 85-106. DOI: 10.5697/oc.56-1.085.

Winn, K. & Averdieck, F.-R. (1984). Post-Boreal development of the Western Baltic: comparison of two local sediment basins. *Meyniana* 36: 35-50.

Witkowski, A., Broszinski, A., Bennike, O., Janczak-Kostecka, B., Bo Jensen, J. et al. (2005). Darss Sill as a biological border in the fossil record of the Baltic Sea: evidence from diatoms. *Quat. Int.* 130: 97-109. DOI: 10.1016/j.quaint.2004.04.035.

Zhang, J., Tsukamoto, S., Grube, A. & Frechen, M. (2014). OSL and 14 C chronologies of a Holocene sedimentary record (Garding-2 core) from the German North Sea coast. *Boreas* 43: 856-868. DOI: 10.1111/bor.12071.